Steel and Composite Structures, *Vol. 39, No. 6 (2021) 765-779*
DOI: https://doi.org/10.12989/scs.2021.39.6.765

Mixed mode I/II fracture criterion to anticipate cracked composite materials based on a reinforced kinked crack along maximum shear stress path

Sadra Shahsavar[1], Mahdi Fakoor*[1] and Filippo Berto[2]

[1]*Faculty of New Sciences and Technologies, University of Tehran, Tehran, Iran*
[2]*Norwegian University of Science and Technology, Norway*

(*Received November 4, 2020, Revised May 10, 2021, Accepted May 18, 2021*)

Abstract. In this paper, a fracture criterion for predicting the failure of the cracked composite specimens under mixed mode I/II loading is provided. Various tests performed on composite components reveal that cracks always grow along the fibers in the isotropic media. Using a new material model called reinforcement isotropic solid (RIS) concept, it is possible to extend the isotropic mixed mode fracture criteria into composite materials. In the proposed criterion, maximum shear stress (MSS) theory which is widely used for failure investigation of un-cracked isotropic materials will be extended to composite materials in combination with RIS concept. In the present study, cracks are oriented along the fibers in the isotropic material. It is assumed that at the onset of fracture, crack growth will be in a path where the shear stress has the highest value according to the MSS criterion. Investigating the results of this criterion and comparing with the available experimental data, it is shown that, both the crack propagation path and the moment of crack growth are well predicted. Available mixed mode I/II fracture data of various wood species are used to evaluate and verify the theoretical results.

Keywords: extended maximum shear stress path; fracture criterion; mixed mode I/II loading; composite materials; reinforcement isotropic solid model; RIS concept; crack growth

1. Introduction

Nowadays, composite structures are widely used in various industries due to their unique properties. These materials are usually subjected to mixed I/II loading during their lifetime (Altunisik *et al.* 2017). Therefore, before utilizing composite materials in any industry, we need to know their failure behavior. One of the main factors in increasing the rate of failure in orthotropic materials is the creation of different defeats in their structure (Fakoor and Ghoreishi 2018). As a result, it is necessary to achieve an efficient failure criterion that can predict crack initiation and propagation in these materials (Wu 1967). For this purpose, numerous studies have been conducted theoretically and experimentally, and several criteria have been proposed. Fakoor and Shahsavar (2020) conducted a comprehensive review of the proposed models and criteria. A succinct review has been conducted on local approaches for the failure assessment of quasi-brittle and brittle materials (Berto 2014). Mixed mode I/II fracture criteria for cracked orthotropic materials, can be classified as shown in Fig. 1.

Preliminary studies on fracture of composite materials have been done experimentally based on curve-fitting on experimental data of different wood species. For the first time, experimental results of balsa wood and glass-fiber reinforced composites have been utilized to provide a mixed mode I/II failure criterion for orthotropic materials (Wu 1967). Mc Kinney (1972) proposed an experimental criterion by performing some tests on single-directional graphite-epoxy composites, utilizing the least squares curve fitting method. In another research, a new empirical criterion based on curve fitting has been proposed using test results of Baltic red wood with cracks in RL direction (Hunt and Croager 1982). Mall *et al.* (1983) used central and edge cracked specimens of Eastern red spruce wood to investigate fracture behavior of orthotropic materials under mixed mode loading and finally, they introduced the appropriate mixed mode I/II experimental criterion. Leicester (2006) employed pine wood in his study and proposed a conservative criterion. Reynolds *et al.* (2019) studied experimentally on fracture of bamboo wood with LR, RL and TL crack under pure mode I and II loading. Chen *et al.* (2011) also experimentally studied on the shear-bond failure mechanism of composite deck slabs.

Empirical criteria have two or three constants that should be evaluated for any specific kinds of materials and this issue is a drawback for them. Therefore, it can be said that these types of criteria, despite accuracy, are very costly and time-consuming (Al-Fasih *et al.* 2018). Fernandino *et al.* (2020) using tensile tests and the specimen's surface observation with SEM, studied on damage evolution at the microstructural scale of a ductile iron partially austenitized. They show that at the onset of fracture, cracks initiate and propagate at the matrix-nodule interface, and then by increasing the load, the initiation and propagation in the metallic matrix take place inside the ausferritic areas. D'Angela *et al.* (2020) also investigated the damaging micro-mechanisms in a pearlitic ductile cast iron specimen

*Corresponding author, Professor
E-mail: mfakoor@ut.ac.ir

ISSN: 1229-9367 (Print), 1598-6233 (Online)

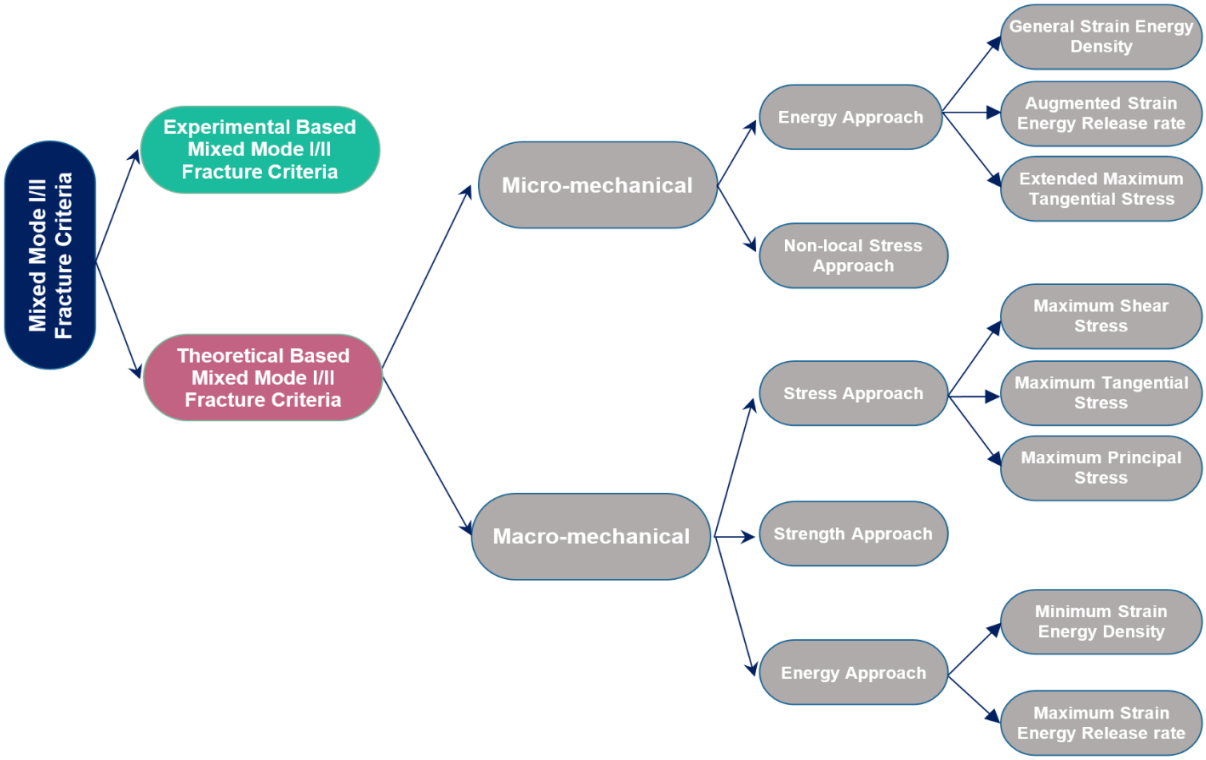

Fig. 1 Mixed mode I/II fracture criteria for cracked orthotropic materials

using SEM analysis and acoustic emission testing.

In another study, Di Cocco *et al.* (2014, 2010) investigated the damaging micro-mechanisms in a ferritic ductile cast iron using SEM with a micro tensile holder in which these tests were performed according to a step by step experimental procedure. Fernandino *et al.* (2020a) also using digital image correlation technique and tensile loading, studied on the damage analysis of the same material. They claimed that cracks initiate in the metallic matrix at the boundary between ausferrite sheaves and propagate at the direction of the ausferrite plates. They also obtained the relation between microstructural heterogeneities and damage mechanisms of a ferritic spheroidal graphite cast iron during tensile loading and examined the crack initiation and propagation of the mentioned specimen (Fernandino *et al.* 2020b, c). Ataabadi *et al.* (2012) studied on the failure models and fiber-kinking of laminated composites under mode I and mode II loading conditions. In another research, some failure criteria have been investigated to predict damage in glass/polyester composite beams under low-velocity impact conditions (Aghaie *et al.* 2015). Rizov (2017) studied the delamination of an end-loaded split functionally graded beam under mode II loading considering material non-linearity by theoretical approach.

Some researches have been done for improving fracture properties of civil and construction materials under a different type of loading (Golewski 2017a, b, c), using microscopic approaches and fracture behavior of composite material, the fracture toughness's of mode I and II have been obtained (Golewski 2018, Golewski *et al.* 2019a, b, Golewski 2019) of composite structures. He also utilized low calcium fly ash in concrete composite and investigated the influence of the curing time on its fracture toughness (Golewski 2020). The behavior of ternary concretes after incorporating Fly Ash and Silica Fume has been investigated (Golewski *et al.* 2021). Also, Golewski (2021) subjected the dynamic load on concrete composite with the addition of fly ash (FA) in the amounts of 0%, 20%, and 30% to investigate the micro-cracks of concrete.

In another study, a model for investigating the non-linear behavior of steel-concrete composite beams has also been proposed (Dall'Asta *et al.* 2002).

In the field of fracture of orthotropic materials, theoretical criteria have been presented with acceptable accuracy based on the extension of well-known isotropic failure criteria such as maximum tangential stress (MTS), maximum principal stress (MPS), maximum shear stress (MSS), strain energy density (SED) and strain energy release rate (SER). For example, MTS and SED criteria have been extended to orthotropic materials to obtain fracture limit curves (FLC's) for predicting crack initiation and propagation (Saouma *et al.* 1987, Nobile *et al.* 2004). Fakoor and Rafiee (2013) using the maximum shear stress criterion which is applicable for failure investigation of isotropic materials, proposed a new mixed mode I/II criterion for fracture assessment of orthotropic materials.

Based on the other well-known isotropic failure theories (MPS, SED, and SER), new mixed mode I/II failure criteria have been introduced by (Jernkvist 2001a). The applicability of these criteria was evaluated by testing on SENT and DCB test specimens made from Norway spruce wood species (Jernkvist 2001b).

Table 1 Some famous theoretical mixed mode I/II loading criteria for orthotropic material

Author	Approach	Theoretical base	Fracture criterion	Damage parameter
Jernkvist (2001a)	LEFM-Approach	SER	$K_I^2+\beta_1 K_{II}^2-K_{IC}^2=0$	$\beta_1=\left(\frac{S'_{11}}{S'_{22}}\right)^{\frac{1}{2}}=\left(\frac{E_I}{E_{II}}\right)$
Jernkvist (2001)		SED	$K_I^2+\beta_2 K_{II}^2-K_{IC}^2=0$	$\beta_2=\frac{S'_{66}\,g_{12}^2(0)}{S'_{11}\,f_{11}^2(0)+S'_{22}\,f_{22}^2(0)+2S'_{12}\,f_{11}(0)\,f_{22}(0)}$
Jernkvist (2001)		MPS	$\frac{1}{(\beta_3+\sqrt{\beta_4})}\left[\beta_3 K_I+\sqrt{\beta_4 K_I^2+K_{II}^2}\right]=K_{IC}$	$\beta_3=\frac{f_{11}(0)+f_{22}(0)}{2}$ *and* $\beta_4=\left(\frac{f_{11}(0)-f_{22}(0)}{2}\right)^2$
Anaraki *et al*. (2010a, b)	RIS-Based approach	Micro-mechanical RIS-approach	$K_I{}^2+\rho_3 K_{II}{}^2=K_{IC}{}^2$	$\rho_3=\frac{(5-\nu)\left(\xi\sqrt{\lambda}+\nu_{LR}\lambda\right)^2}{(10-3\nu)(1+0.5+\nu_{LR}(1+\lambda))^2}$
Fakoor (2017)		ASER	$\left(K_I^{ortho}\right)^2+n_1\left(K_{II}^{ortho}\right)^2=\left(K_c^{eq}\right)^2=\left[\frac{1}{2n_1}\left(\sqrt{n_1}-\nu_{xy}+\frac{n_1}{2n_6}\left(2+\nu_{yx}+\nu_{xy}\right)\right)\right]^{-1/2}\left(K_{Ic}^{ortho}\right)^2$	
Farid *et al*. (2019)		SED	$A_{11}(0)K_I^2+A_{22}(0)K_{II}^2=A_{11}(0)\left(K_{Ic}\right)^2$	$\rho_6=\frac{C_{66}}{n_6^2\left(\frac{C_{11}}{n_1^2}+\frac{C_{22}}{n_2^2}+2\frac{C_{12}}{n_1 n_2}\right)}$
Fakoor and Farid (2019)		GSED	$A_{11}(\varphi)K_I^2+2A_{12}(\varphi)K_I K_{II}+A_{22}(\varphi)K_{II}^2+A_{13}(\varphi)K_I+A_{23}(\varphi)K_{II}+A_{33}=A_{11}(0)K_{Ic}^2$	
Shahsavar *et al*. (2020)		MSS (crack along the fibers)	$K_I^2+\frac{K_{II}^2}{\rho_2\,\xi_3^2}=K_{Ic}^2$	$\rho_2=\left(\frac{f_{11}(0)-\xi_1 f_{22}(0)}{2\xi_1}\right)^2$
Shahsavar *et al*. (2020)		MSS (crack across the fiber)	$\left(\alpha_{11}K_I+\alpha_{12}K_{II}\right)^2+\frac{1}{\xi_3\rho_3}\left(\alpha_{21}K_I+\alpha_{22}K_{II}\right)^2=K_{Ic}^2$	$\rho_3=\left(\frac{f_{11}(0)-\xi_1 f_{22}(0)}{2\xi_1}\right)^2$

He concluded that these extended criteria are acceptable just for dominant mode I conditions, i.e. K_I and energy-based criteria (i.e., SER and SED) were conservative due to the assumption of linear elastic fracture mechanics (Jernkvist 2001b). Numerical analysis of center cracked orthotropic FGM plate has been conducted and the mode I stress intensity factors at the crack tips has been calculated using the Displacement Correlation Method (Kaman and Cetisli 2012).

Another approach based on the non-local stress criterion was adopted to investigate the fracture of orthotropic materials for the case of cracks oriented with arbitrary angles with respect to the fibers (Romanowicz and Seweryn 2008). This approach was compared with the MTS criterion and concluded that the non-local stress concept is more accurate than MTS (Romanowicz 2019). Considering non-singular T-stress term and FPZ effects, a new mixed mode fracture criterion for composite materials has been presented (Anaraki and Fakoor 2010, 2011). Also, introducing a representative circle element (RCE) model and effective elastic properties of a damage zone around the crack tip has been obtained (Fakoor and Khansari 2016).

Using the Van der Put's theory (Van der Put 2007), a new concept which was named the "reinforcement isotropic solid" (RIS) model for fracture investigation of orthotropic materials was proposed by Fakoor *et al.* (Fakoor 2017, Fakoor and Khansari 2018, Fakoor *et al.* 2019). RIS assumes orthotropic materials as an isotropic solid media which is reinforced with the fibers. Employing the RIS concept, well-known isotropic fracture criteria such as SED, MTS, and SER were extended to orthotropic materials. They also verified their proposed concept with different failure theories and experimental test results (Khansari *et al.* 2019, Farid *et al*. 2019, Fakoor and Farid 2019, Farid *et al.* 2020, Shahsavar *et al.* 2020).

As a conclusion, the most famous theoretical mixed mode I/II fracture criteria are summarized in Table 1.

The purpose of the present research is to find a mixed mode I/II fracture criterion for fracture assessment of highly orthotropic materials. As discussed in the literature, several theories have been proposed for predicting mixed mode fracture in orthotropic materials with quasi-brittle behavior based on well-known isotropic fracture criteria (i.e., MTS, MPS, SED, SER, and so on). In nearly all proposed criteria, crack propagation direction is assumed to be along the

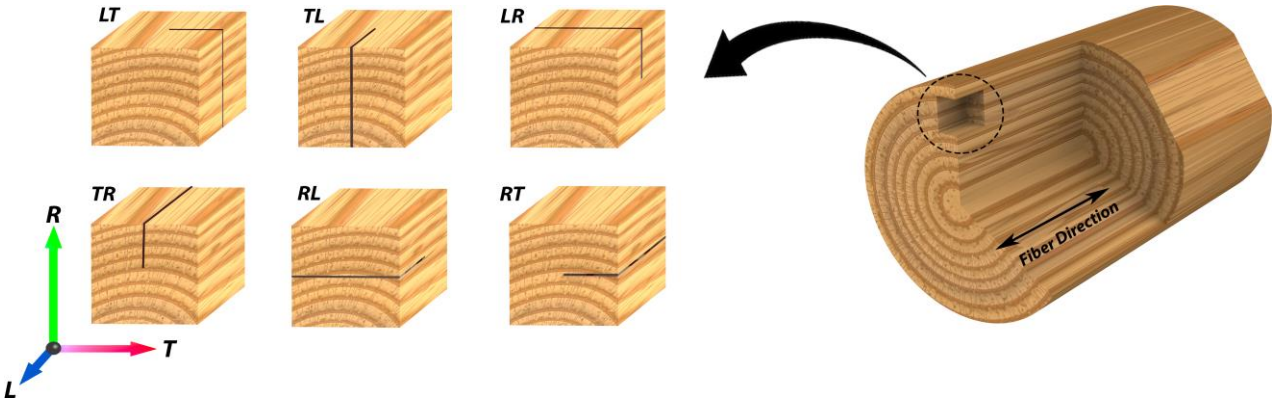

Fig. 2 Six possible crack growth systems in wood species

Table 2 Elastic modulus and fracture properties of wood specimens employed in this study (GPa)

Wood Species Name	E_R	E_T	E_L	G_{RL}	ν_{LR}	ν_{LT}	ν_{TR}	K_{Ic}^{RL}	K_{IIc}^{RL}	K_{Ic}^{TL}	K_{IIc}^{TL}
Norway spruce (Picea abies) (Jernkvist 2001b, Edlund *et al.* 2006)	0.81	0.64	11.84	0.63	0.38	0.56	0.34	0.58	1.52	-	-
Scots pine (Pinus sylvestris) (Kollmann *et al.* 2006)	1.10	0.57	16.3	1.74	0.47	0.45	0.31	0.49	1.32	0.44	2.05
Red spruce (Picea rubens) (Ross 2010)	098	0.63	12.7	0.80	0.37	0.42	0.30	0.42	1.66	0.42	2.19

fibers with a self-similar assumption.

Although this assumption may be acceptable from a microscopic point of view, detail microscopic observations of the crack tip at the crack propagation moment, reveals a crack kinking phenomenon between the fibers. In the presentation of the new mixed mode fracture criterion, this kinking phenomenon is taken into account utilizing the reinforcement isotropic solid (RIS) concept. In the RIS concept, the effect of fibers on the matrix in orthotropic materials is modeled via reinforcement or stress reduction coefficients. Then the well-known maximum shear stress (MSS) theory is employed to anticipate the kink angle and onset of in-plane crack propagation. The superiority of the present work is proven with the comparison of the derived fracture limit curves by available experimental data.

2. Theoretical background and problem statement

2.1 Materials and assumptions

In this research, wood as a natural highly orthotropic material is utilized for the case study. It has been shown that due to the complex structure of wood components and the inherent defects, any fracture criterion that can interpret the behavior of wood failure is certainly able to predict the failure in man-made composite materials (Fakoor and Shahsavar 2020, Wang *et al.* 2019). Wood has special mechanical properties in different directions wherein its three principal directions are longitudinal (L), tangential (T) and radial (R). These three principal directions and the six possible crack growth systems are shown in Fig. 2. In this paper, the behavior of most probable crack systems (i.e., RL and TL) in which cracks are oriented along the fibers is investigated. Mixed mode I/II loading and plane strain conditions are assumed in the theoretical analysis. Elastic properties and fracture toughness of the wood species studied in this paper are also summarized in Table 2.

2.2 Stress field in the vicinity of the crack tip in orthotropic material

The stress state near the crack tip of an orthotropic body is illustrated in Fig. 3.

The corresponding stress components are defined as follows

$$\sigma_{ij}=\frac{K_I}{\sqrt{2\pi r}}f_{ij}(\theta)+\frac{K_{II}}{\sqrt{2\pi r}}g_{ij}(\theta);\quad i,j=1,2 \tag{1}$$

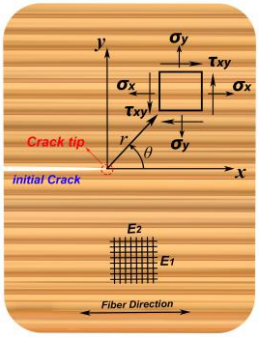

Fig. 3 Crack tip stress state

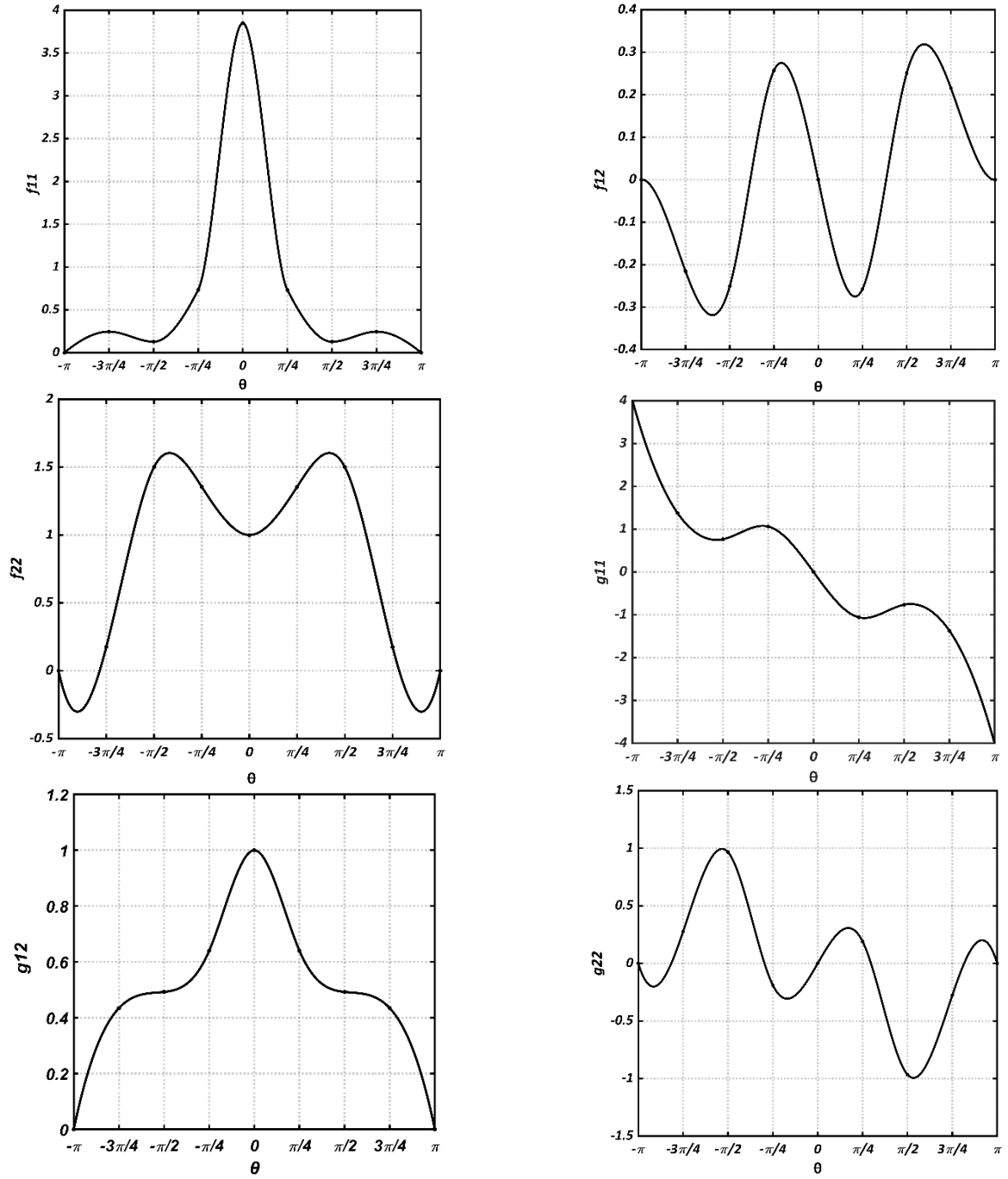

Fig. 4 Dependency of f_{ij} and g_{ij} to crack growth path in Scots pine sample

In the above equation $f_{ij}(\theta)$ and $g_{ij}(\theta)$ are the material-dependent angular functions. For orthotropic materials, these parameters are as follows (Sih *et al*. 1965)

$$f_{11}(\theta)=\mathrm{Re}\left[\frac{\vartheta_1\vartheta_2(\vartheta_2\delta_2-\vartheta_1\delta_1)}{\vartheta_1-\vartheta_2}\right]$$
$$f_{22}(\theta)=\mathrm{Re}\left[\frac{\vartheta_1\delta_2-\vartheta_2\delta_1}{\vartheta_1-\vartheta_2}\right] \quad (2a)$$

$$g_{11}(\theta)=\mathrm{Re}\left[\frac{(\vartheta_2^2\delta_2-\vartheta_1^2\delta_1)}{\vartheta_1-\vartheta_2}\right]$$
$$g_{11}(\theta)=\mathrm{Re}\left[\frac{(\vartheta_2^2\delta_2-\vartheta_1^2\delta_1)}{\vartheta_1-\vartheta_2}\right] \quad (2b)$$
$$g_{22}(\theta)=\mathrm{Re}\left[\frac{\delta_2-\delta_1}{\vartheta_1-\vartheta_2}\right]$$
$$g_{12}(\theta)=\mathrm{Re}\left[\frac{(\vartheta_1\delta_1-\vartheta_2\delta_2)}{\vartheta_1-\vartheta_2}\right]$$

Where, δ_1 and δ_2 are defined as follows

$$\delta_1 = \frac{1}{\left(\cos\theta + \vartheta_1 \sin\theta\right)^{1/2}}, \quad \delta_2 = \frac{1}{\left(\cos\theta + \vartheta_2 \sin\theta\right)^{1/2}} \tag{3}$$

ϑ_1 and ϑ_2 are the roots of the following characteristic equation (Su and Sun 2003)

$$C_{11}\vartheta^4 + 2C_{16}\vartheta^3 + \left(2C_{12} + C_{66}\right)\vartheta^2 - 2C_{26}\vartheta + C_{22} = 0 \tag{4}$$

In the above equation C_{ij}' are the components of the below compliance matrix

$$\begin{pmatrix} \varepsilon_{11} \\ \varepsilon_{22} \\ \varepsilon_{33} \\ \gamma_{23} \\ \gamma_{31} \\ \gamma_{12} \end{pmatrix} = \begin{pmatrix} 1/E_1 & -\nu_{21}/E_2 & -\nu_{31}/E_3 & 0 & 0 & 0 \\ -\nu_{12}/E_1 & 1/E_2 & -\nu_{32}/E_3 & 0 & 0 & 0 \\ -\nu_{13}/E_1 & -\nu_{23}/E_2 & 1/E_2 & 0 & 0 & 0 \\ 0 & 0 & 0 & 1/G_{23} & 0 & 0 \\ 0 & 0 & 0 & 0 & 1/G_{31} & 0 \\ 0 & 0 & 0 & 0 & 0 & 1/G_{12} \end{pmatrix} \begin{pmatrix} \sigma_{11} \\ \sigma_{22} \\ \sigma_{33} \\ \tau_{23} \\ \tau_{31} \\ \tau_{12} \end{pmatrix} \tag{5}$$

For plane strain conditions, the following equation is used for components of the compliance matrix

$$C'_{ij} = C_{ij} - C_{i3}C_{j3}/C_{33} \quad (i, j = 1, 2) \tag{6}$$

$f_{ij}(\theta)$ and $g_{ij}(\theta)$ can lead us to a possible fracture plane at crack tip vicinity. Fig. 4 reveals the dependency of f_{ij} and g_{ij} to crack growth path in Scots pine wood species.

The cracking tendency to grow along the maximum shear stress plane in isotropic matrix among the fibers has been investigated in Appendix A.

3. Deriving the mixed mode I / II fracture criteria

3.1 Augmented maximum shear stress fracture criterion (AMSS)

Considering the orthotropic stress field, the well-known and practical MSS theory is used to study the fracture behavior of orthotropic materials under mixed-mode I/II loading (Fakoor and Rafiee 2013). Tresca stress theory which is applicable for failure assessment of isotropic materials is defined as follows

$$\tau_{\max} = \sqrt{\frac{1}{4}\left(\sigma_{11}^2 + \sigma_{22}^2 - 2\sigma_{11}\sigma_{22}\right) + {\sigma_{12}}^2} \tag{7}$$

According to the stress state at the crack tip of orthotropic material (Eq. (1)), the following relations can be defined

$$\sigma_{11}^2 = \frac{1}{2\pi r}\left(f_{11}^2 K_I^2 + g_{11}^2 K_{II}^2 + 2 f_{11} g_{11} K_I K_{II}\right) \tag{8}$$

$$\sigma_{22}^2 = \frac{1}{2\pi r}\left(f_{22}^2 K_I^2 + g_{22}^2 K_{II}^2 + 2 f_{22} g_{22} K_I K_{II}\right)$$

$$\sigma_{12}^2 = \frac{1}{2\pi r}\left(f_{12}^2 K_I^2 + g_{12}^2 K_{II}^2 + 2 f_{12} g_{12} K_I K_{II}\right)$$

$$\sigma_{11}\sigma_{22} = \frac{1}{2\pi r}\left(\begin{array}{l} f_{11}g_{22}K_I^2 + f_{11}g_{22}K_{II}^2 + \\ \qquad \left(f_{11}g_{22} + f_{22}g_{11}\right)K_I K_{II} \end{array}\right)$$

Through substituting Eq. (8) into Eq. (7), we have the following from for MSS

$$\tau_{\max} = \left(A_{11}K_I^2 + A_{12}K_I K_{II} + A_{22}K_{II}^2\right)^{1/2} \tag{9}$$

In which A_{ij} coefficients are defined as follows

$$A_{11} = \frac{1}{2\pi r}\left(\frac{f_{11}^2}{4} + \frac{f_{22}^2}{4} - \frac{f_{11}f_{22}}{2} + f_{12}^2\right)K_I^2$$

$$A_{12} = \frac{1}{2\pi r}\left(\frac{f_{11}g_{11}}{2} + \frac{f_{22}g_{22}}{2} - \frac{(f_{11}g_{22} + f_{11}g_{22})}{2} + 2 f_{12}g_{12}\right)K_{II}K_I \tag{10}$$

$$A_{22} = \frac{1}{2\pi r}\left(\frac{q_{11}^2}{4} + \frac{g_{22}^2}{4} - \frac{g_{11}g_{22}}{2} + g_{12}^2\right)K_{II}^2$$

Crack propagation is assumed to be when $\tau_{\max} = \tau_{cr}$, considering crack propagation along the fibers (i.e. $K_{II} = 0$, $K_I = K_{Ic}$), the critical value of maximum shear stress (τ_{cr}) for crack propagation can be obtained as follows

$$\tau_{cr} = \frac{K_{Ic}}{\sqrt{2\pi r}}\left(\frac{f_{11} - f_{22}}{2}\right) \tag{11}$$

Now for self-similar crack propagation, the final form of AMSS fracture criterion for cracks along the fibers ($\varphi = 0$) is (Shahsavar *et al*. 2020)

$$K_I^2 + \frac{1}{\psi_1}K_{II}^2 = K_{Ic}^2 \tag{12}$$

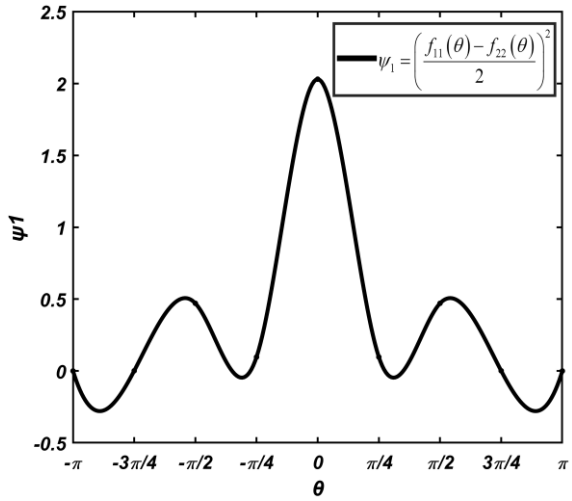

Fig. 5 Dependency of the damage factor (ψ_1) to crack growth path in Scots pine sample

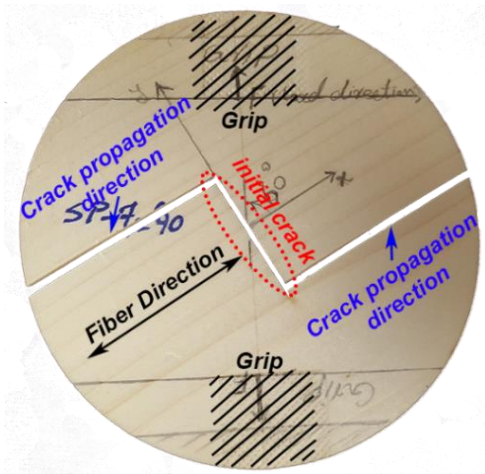

Fig. 6 Crack kinking in an orthotropic material

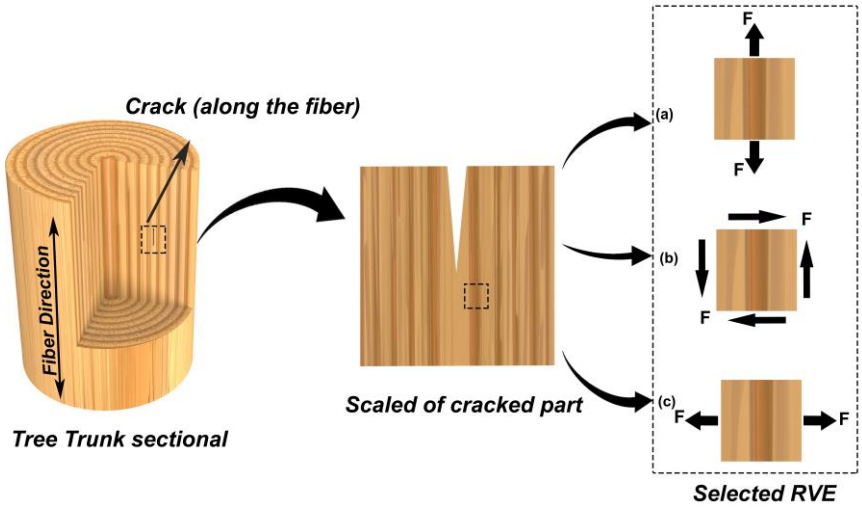

Fig. 7 Selected RVE for extraction of RIS coefficients under (a) tension along the fibers (b) shear loading and (c) tension across the fibers

Where, $\psi_1 = \left(\frac{f_{11}(\theta) - f_{22}(\theta)}{2} \right)^2$, and defines as a damage parameter. Eq. (12) was derived by (Fakoor and Rafiee 2013) by another alternative approach wherein ψ_1 was equal to $\left(K_{Ic} / K_{IIc}\right)^2$, which depends on almost inaccessible mode II fracture toughness of the material.

Fig. 5 depicts the variation of ψ_1 in Scots pine wood for different angles around the crack tip.

As observed in Fig. 5, the maximum value of the damage factor is in the direction of the fibers (i.e. $\theta = 0$) and it is in accordance with the self-propagation assumption of AMSS. Obviously, this curve has different amplitudes for other orthotropic materials, but the overall behavior is the same.

3.2 Reinforcement isotropic solid (RIS) model

According to various experimental observations, crack with any arbitrary direction with respect to the fibers in orthotropic materials kinks immediately after the onset of fracture and propagates along the fibers in the isotropic matrix (See Fig. 6).

For the case of Fig. 7(a), fibers and matrix tolerate the applied load simultaneously, in which the fibers increase the strength of the material in their direction. But, in the case of Fig. 7(c), the fibers do not contribute to load-bearing and therefore do not have significant effects in stress reduction of the matrix media; thus, the RIS-factors of this case are equal to one. As a result, the RIS-factors can be defined as follows (Fakoor and Farid 2019)

$$\gamma_1 = \frac{E_{xx}}{E_{yy}} \quad \gamma_2 = 1 \quad \gamma_3 = \left(1 - V_f\right)\left(1 + \frac{E_{11}\left(1+\upsilon_{21}\right)}{E_{22}\left(1+\upsilon_{12}\right)}\right) \tag{13}$$

The stress state at the crack tip of the isotropic matrix is as follows

$$\sigma_{ij}=\frac{K_I}{\sqrt{2\pi r}}p_{ij}(\theta)+\frac{K_{II}}{\sqrt{2\pi r}}q_{ij}(\theta)\quad ,(i,j=1,2) \tag{14}$$

Therefore, using RIS-factors, an orthotropic stress state can be converted to a reinforced isotropic stress state employing the following relations

In the RIS model, orthotropic material is assumed as an equivalent isotropic media which is reinforced with fibers as reinforcing elements. The fibers are more potent than the matrix and tolerate most of the subjected load. Therefore, the crack cannot tear the fibers and propagates in the weak plane of the isotropic matrix. In the RIS concept, isotropic and orthotropic stress fields are related to each other with some coefficients named as "stress reduction" or "RIS" factors (Fakoor and Farid 2019, Daneshjoo *et al*. 2018). The significant superiority of this manner is considering the effect of the volume fraction of fibers in a stress state. They selected a suitable RVE as shown in Fig. 7 to obtain RIS-factors with FEA software.

$$\sigma'_{11}=\frac{K_I}{\gamma_1\sqrt{2\pi r}}p_{11}(\theta)+\frac{K_{II}}{\gamma_1\sqrt{2\pi r}}q_{11}(\theta) \tag{15}$$

$$\sigma'_{22}=\frac{K_I}{\gamma_2\sqrt{2\pi r}}p_{22}(\theta)+\frac{K_{II}}{\gamma_2\sqrt{2\pi r}}q_{22}(\theta)$$

$$\sigma'_{12}=\frac{K_I}{\gamma_3\sqrt{2\pi r}}p_{12}(\theta)+\frac{K_{II}}{\gamma_3\sqrt{2\pi r}}q_{12}(\theta)$$

Where, σ'_{ij} is the stress state at the crack tip in the reinforced matrix and also p_{ij} and q_{ij} represent the angular functions of isotropic stress state which are defined as follows (Williams 1961)

$$\begin{aligned}
p_{11}(\theta)&=(\cos\frac{\theta}{2})(1-\sin\frac{3\theta}{2}\sin\frac{\theta}{2})\\
p_{22}(\theta)&=(\cos\frac{\theta}{2})(1+\sin\frac{3\theta}{2}\sin\frac{\theta}{2})\\
p_{12}(\theta)&=\sin\frac{\theta}{2}\cos\frac{\theta}{2}\cos\frac{3\theta}{2}\\
q_{11}(\theta)&=(\sin\frac{\theta}{2})(2+\cos\frac{3\theta}{2}\cos\frac{\theta}{2})\\
q_{22}(\theta)&=\sin\frac{\theta}{2}\cos\frac{\theta}{2}\cos\frac{3\theta}{2}\\
q_{12}(\theta)&=(\cos\frac{\theta}{2})(1-\sin\frac{3\theta}{2}\sin\frac{\theta}{2})
\end{aligned} \tag{16}$$

3.3 Generalized maximum shear stress fracture criterion in combination with RIS concept (RIS-GMSS)

On the contrary to previous studies, experimental tests on wooden materials demonstrate that at the onset of fracture, in microscopic point of view, oriented crack along the fibers in the matrix of orthotropic lamina starts to deflect and grows in a different direction (i.e., θ_c) (Farid *et al.* 2020). This phenomenon is schematically shown in Fig. 8. In this section to establish the RIS-GMSS criterion, crack growth will be examined in the direction in which shear stress has the highest value based on the MSS criterion.

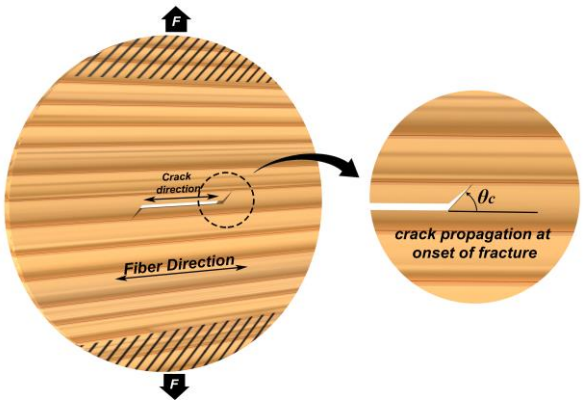

Fig. 8 Crack propagation direction at the onset of fracture in microscopic point of view

According to RIS concept and Eq. (15), the following relations where included RIS-factors are defined

$$\begin{aligned}
\sigma'^2_{11}&=\frac{1}{2\pi r}\left(\frac{p_{11}^2K_I^2+q_{11}^2K_{II}^2+2p_{11}q_{11}K_IK_{II}}{\gamma_1^2}\right)\\
\sigma'^2_{22}&=\frac{1}{2\pi r}\left(\frac{p_{22}^2K_I^2+q_{22}^2K_{II}^2+2p_{22}q_{22}K_IK_{II}}{\gamma_2^2}\right)\\
\sigma'^2_{12}&=\frac{1}{2\pi r}\left(\frac{p_{12}^2K_I^2+q_{12}^2K_{II}^2+2p_{12}q_{12}K_IK_{II}}{\gamma_3^2}\right)\\
\sigma'_{11}\sigma'_{22}&=\frac{1}{2\pi r}\left(\frac{p_{11}p_{22}K_I^2+q_{11}q_{22}K_{II}^2+(p_{11}q_{22}+p_{22}q_{11})K_IK_{II}}{\gamma_1\gamma_2}\right)
\end{aligned} \tag{17}$$

Therefore, according to Tresca theory, the new form of $\tau_{\max}$ including reinforcement factors is defined as follows

$$\tau_{\max}=\left[A_{11}^{RIS}K_I^2+A_{12}^{RIS}K_IK_{II}+A_{22}^{RIS}K_{II}^2\right]^{\frac{1}{2}} \tag{18}$$

In which A_{ij}^{RIS} factors are defined as follows

$$\begin{aligned}
A_{11}^{RIS}&=\frac{1}{2\pi r}\left(\frac{p_{11}^2}{4\gamma_1^2}+\frac{p_{22}^2}{4\gamma_2^2}-\frac{p_{11}p_{22}}{2\gamma_1\gamma_2}+\frac{p_{12}^2}{\gamma_3^2}\right)\\
A_{12}^{RIS}&=\frac{1}{2\pi r}\left(\frac{p_{11}q_{11}}{2\gamma_1^2}+\frac{p_{22}q_{22}}{2\gamma_2^2}-\frac{(p_{11}q_{22}+p_{22}q_{11})}{2\gamma_1\gamma_2}+\frac{2p_{12}q_{12}}{\gamma_3^2}\right)\\
A_{22}^{RIS}&=\frac{1}{2\pi r}\left(\frac{q_{11}^2}{4\gamma_1^2}+\frac{q_{22}^2}{4\gamma_2^2}-\frac{q_{11}q_{22}}{2\gamma_1\gamma_2}+\frac{q_{12}^2}{\gamma_3^2}\right)
\end{aligned} \tag{19}$$

In order to obtain RIS-GMSS criterion, the following assumptions are considered:

- The crack grows in the isotropic matrix of orthotropic material.
- Crack tip stresses are considered with RIS coefficients in the isotropic matrix stress field.
- Crack propagates in the direction that the

maximum shear stress reaches its critical value.

- Crack direction changes after contact with the fibers (crack kinking phenomenon) and propagates along the fibers

Considering the above assumptions, Eqs. (17) to (19) are employed to establish the RIS-GMSS criterion. According to the MSS criterion, the crack propagates when the critical shear stress reaches its maximum value at a critical distance; thus, the following three conditions must be met simultaneously to obtain the desired criterion

$$\tau_{\max}=\left(\tau_{\max}\right)_{cr} \quad , \quad \frac{\partial\tau_{\max}}{\partial\theta}=0 \quad , \quad \frac{\partial^2\tau_{\max}}{\partial\theta^2}<0 \qquad (20)$$

The first condition is to get the maximum critical shear stress $\left(\tau_{\max}\right)_{cr}$. As mentioned, this value is part of the properties of the material. The pure mode I loading conditions (i.e. $\theta_C=0, K_{II}=0, K_I=K_{Ic}$), are employed to express the $\left(\tau_{\max}\right)_{cr}$ as a function of the mode I fracture toughness.

The first condition is to get the maximum critical shear stress $\left(\tau_{\max}\right)_{cr}$. As mentioned, this value is part of the properties of the material. The pure mode I loading conditions (i.e. $\theta_C=0, K_{II}=0, K_I=K_{Ic}$), are employed to express the $\left(\tau_{\max}\right)_{cr}$ as a function of the mode I fracture toughness.

The second and third conditions specify the crack growth path, which is calculated as follows

$$\frac{\partial\tau_{\max}}{\partial\theta}=0 \Rightarrow \left(A'_{11}\right)^{RIS}K_I^2+\left(A'_{12}\right)^{RIS}K_IK_{II}+\left(A'_{22}\right)^{RIS}K_{II}^2=0 \qquad (21)$$

Where

$$\left(A'_{11}\right)^{RIS}=\frac{1}{2\pi r}\left(\begin{array}{l}\dfrac{2p_{11}p'_{11}}{4\gamma_1^2}+\dfrac{2p_{22}p'_{22}}{4\gamma_2^2}-\\ \dfrac{\left(p'_{11}p_{22}+p_{11}p'_{22}\right)}{2\gamma_1\gamma_2}+\dfrac{2p_{12}p'_{12}}{\gamma_3^2}\end{array}\right)$$

$$\left(A'_{12}\right)^{RIS}=\frac{1}{2\pi r}\left(\begin{array}{l}\dfrac{\left(p'_{11}q_{11}+p_{11}q'_{11}\right)}{2\gamma_1^2}+\dfrac{\left(p'_{22}q_{22}+p_{22}q'_{22}\right)}{2\gamma_2^2}-\\ \dfrac{\left(\left(p'_{11}q_{22}+p_{11}q'_{22}\right)+\left(p'_{22}q_{11}+p_{22}q'_{11}\right)\right)}{2\gamma_1\gamma_2}+\\ \dfrac{2\left(p'_{12}q_{12}+p_{22}q'_{11}\right)}{\gamma_3^2}\end{array}\right) \qquad (22)$$

$$\left(A'_{22}\right)^{RIS}=\frac{1}{2\pi r}\left(\begin{array}{l}\dfrac{2q_{11}q'_{11}}{4\gamma_1^2}+\dfrac{2q_{22}q'_{22}}{4\gamma_2^2}-\\ \dfrac{\left(q'_{11}q_{22}+q_{11}q'_{22}\right)}{2\gamma_1\gamma_2}+\dfrac{2q_{12}q'_{12}}{\gamma_3^2}\end{array}\right)$$

Regarding the third condition, the below relations are obtained

$$\frac{\partial^2\tau_{\max}}{\partial\theta^2}<0 \Rightarrow \left(A''_{11}\right)^{RIS}K_I^2+\left(A''_{12}\right)^{RIS}K_IK_{II}+\left(A''_{22}\right)^{RIS}K_{II}^2<0 \qquad (23)$$

In which

$$\left(A''_{11}\right)^{RIS}=\frac{1}{2\pi r}\left(\begin{array}{l}\dfrac{2\left(p'^2_{11}+p_{11}p''_{11}\right)}{4\gamma_1^2}+\dfrac{2\left(p'^2_{22}+p_{22}p''_{22}\right)}{4\gamma_2^2}-\\ \dfrac{\left(\left(p''_{11}p_{22}+p'_{11}p'_{22}\right)+\left(p'_{11}p'_{22}+p_{11}p''_{22}\right)\right)}{2\gamma_1\gamma_2}\\ +\dfrac{2\left(p'^2_{12}+p_{12}p''_{12}\right)}{\gamma_3^2}\end{array}\right)$$

$$\left(A''_{12}\right)^{RIS}=\frac{1}{2\pi r}\left(\begin{array}{l}\dfrac{\left(\left(p''_{11}q_{11}+p'_{11}q'_{11}\right)+\left(p'_{11}q'_{11}+p_{11}q''_{11}\right)\right)}{2\gamma_1^2}+\\ \dfrac{\left(\left(p''_{22}q_{22}+p'_{22}q'_{22}\right)+\left(f'_{22}g'_{22}+f_{22}g''_{22}\right)\right)}{2\gamma_2^2}-\\ \dfrac{\left(\left(p''_{11}q_{22}+p'_{11}q'_{22}\right)+\left(p'_{11}q'_{22}+p_{11}a''_{22}\right)\right)}{2\gamma_1\gamma_2}+\\ \dfrac{\left(\left(p''_{22}q_{11}+p'_{22}q'_{11}\right)+\left(p'_{22}q'_{11}+p_{22}q''_{11}\right)\right)}{2\gamma_1\gamma_2}+\\ \dfrac{2\left(\left(p''_{12}q_{12}+p'_{12}q'_{12}\right)+\left(p'_{22}q'_{11}+p_{22}q''_{11}\right)\right)}{\gamma_3^2}\end{array}\right) \qquad (24)$$

$$\left(A''_{22}\right)^{RIS}=\frac{1}{2\pi r}\left(\begin{array}{l}\dfrac{2\left(q'^2_{11}+q_{11}q''_{11}\right)}{4\gamma_1^2}+\dfrac{2\left(q'^2_{22}+q_{22}q''_{22}\right)}{4\gamma_2^2}-\\ \dfrac{\left(\left(q''_{11}q_{22}+q'_{11}q'_{22}\right)+\left(q'_{11}q'_{22}+q_{11}q''_{22}\right)\right)}{2\gamma_1\gamma_2}+\\ \dfrac{2\left(q'^2_{12}+q_{12}q''_{12}\right)}{\gamma_3^2}\end{array}\right)$$

In this way, utilizing Eqs. (21) to (24), the criterion related to the state of ($\theta_c=\left(\theta_c\right)_{MSS}$) can be obtained as follows

$$A_{11}^{RIS}\left(\theta_c\right)K_I^2+A_{12}^{RIS}\left(\theta_c\right)K_IK_{II}+A_{22}^{RIS}\left(\theta_c\right)K_{II}^2=A_{11}^{RIS}\left(0\right)K_{Ic}^2 \qquad (25)$$

here, the damage parameter of RIS-GMSS criterion (ψ_2) is defined as follows

$$\psi_2=\frac{A_{22}^{RIS}\left(\theta_c\right)}{A_{11}^{RIS}\left(0\right)} \qquad (26)$$

Fig. 9 depicts the variation of ψ_2 around the crack tip for Scots pine wood as a sample. The maximum damage factor occurs at an angle of 45° which is in accordance with the angle of the maximum shear stress plane (See Appendix ***A***).

4. Result and discussion

In order to validate the criteria, experimental data of three types of wood species have been utilized from the literature. Figs. 10(a)-10(c) depicts the fracture limit curves of the proposed criteria in comparison with Scots pine, Norway spruce, and Eastern red spruce experimental data, respectively.

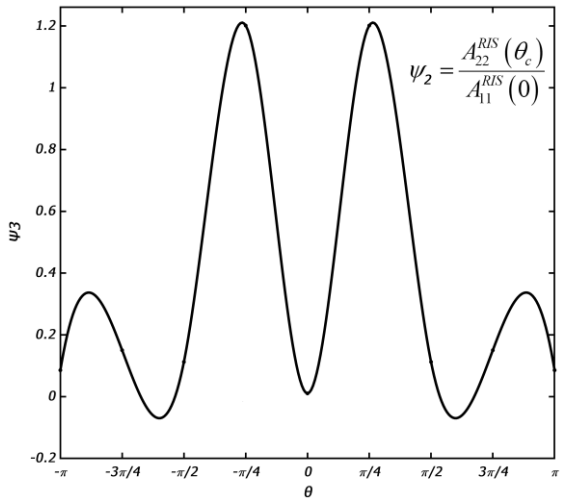

Fig. 9 Dependency of the damage factor (ψ_2) to crack growth path in Scots pine sample

As observed in Fig. 10 more accurate coincidence with experimental data can be found in FLC's of RIS-GMSS criterion. Precise physics-based assumptions such as cracking propagation tendency along with maximum shear stress and employing the reinforcement isotropic model are the main reasons for this accurate estimation. Embedded damage factor in RIS-GMSS criterion (ψ_2), has absolute maximum along the maximum shear stress planes (See Fig. 8 and Appendix A). The aforementioned damage factor includes significant effects of shear stress which is reduced with γ_3. It could be concluded that the maximum shear stress theory is in accordance with the nature of fracture of fibrous composites such as wood.

5. Conclusions

The processes of manufacturing, machining, and forming materials can lead to defects in engineering components, especially composite parts. Neglecting these defects in the designing process, leads to catastrophic failures in the structures. The effects of these cracks and defects can be considered with a suitable failure criterion. In this paper, the RIS-GMSS fracture criterion was derived based on the well-known maximum shear stress failure theory for cracked orthotropic materials wherein crack was oriented along the fibers. Mixed mode I/II loading was considered in this research as general in-plane loading condition. The reinforcement isotropic solid concept (RIS) as a new superior material model was utilized to investigate the fracture of orthotropic materials. In the RIS concept, fibers are assumed as reinforcing elements, which reduce the stress state subjected to the matrix by three defined factors. These factors depend on the elastic properties and the fiber volume fraction of the material. Unlike self-similar crack propagation assumption in available mixed mode fracture criteria, in RIS-GMSS criterion cracking propagation tendency was considered along maximum shear stress. From a microscopic point of view at the onset of fracture, RIS-GMSS assumes that the crack makes a small kink along the MSS in the isotropic matrix medium. Crack propagation was also considered to happen when maximum shear stress reaches its critical value at a critical distance from the crack tip. Accuracy of RIS-GMSS fracture limit curves in the prediction of mixed mode experimental fracture data related to three kinds of wood species proved the superiority of the proposed criterion.

References

Aghaei, M., Forouzan, M.R., Nikforouz, M. and Shahabi, E. (2015), "A study on different failure criteria to predict damage in glass/polyester composite beams under low velocity impact", *Steel Compos. Struct.*, **18**(5), 1291-1303. https://doi.org/10.12989/scs.2015.18.5.1291.

Akbaş, Ş.D. (2019), "Nonlinear behavior of fiber reinforced cracked composite beams", *Steel Compos. Struct.*, **30**(4), 327-336. https://doi.org/10.12989/scs.2019.30.4.327.

Al-Fasih, M.Y., Kueh, A.B.H., Abo Sabah, S.H. and Yahya, M.Y. (2018), "Tow waviness and anisotropy effects on Mode II fracture of triaxially woven composite", *Steel Compos. Struct.*, **26**(2), 241-253. https://doi.org/10.12989/scs.2018.26.2.241.

Altunisik, A.C., Gunaydin, M., Sevim, B. and Adanur, S. (2017), "System identification of arch dam model strengthened with CFRP composite materials", *Steel Compos. Struct.*, **25**(2), 231-244. https://doi.org/10.12989/scs.2017.25.2.231.

Anaraki, A.G. and Fakoor, M. (2010), "General mixed mode I/II fracture criterion for wood considering T-stress effects", *Mater. Design*, **31**(9), 4461-4469. https://doi.org/10.1016/j.matdes.2010.04.055.

Anaraki, A.G. and Fakoor, M. (2011), "A new mixed-mode fracture criterion for orthotropic materials, based on strength properties", *J. Strain Anal. Eng.*, **46**(1), 33-44. https://doi.org/10.1243/03093247JSA667.

Ataabadi, K., Ziaei-Rad, S. and Hosseini-Toudeshky, H. (2012), "Compression failure and fiber-kinking modeling of laminated composites", *Steel Compos. Struct.*, **12**(1), 53-72. http://dx.doi.org/10.12989/scs.2011.12.1.053.

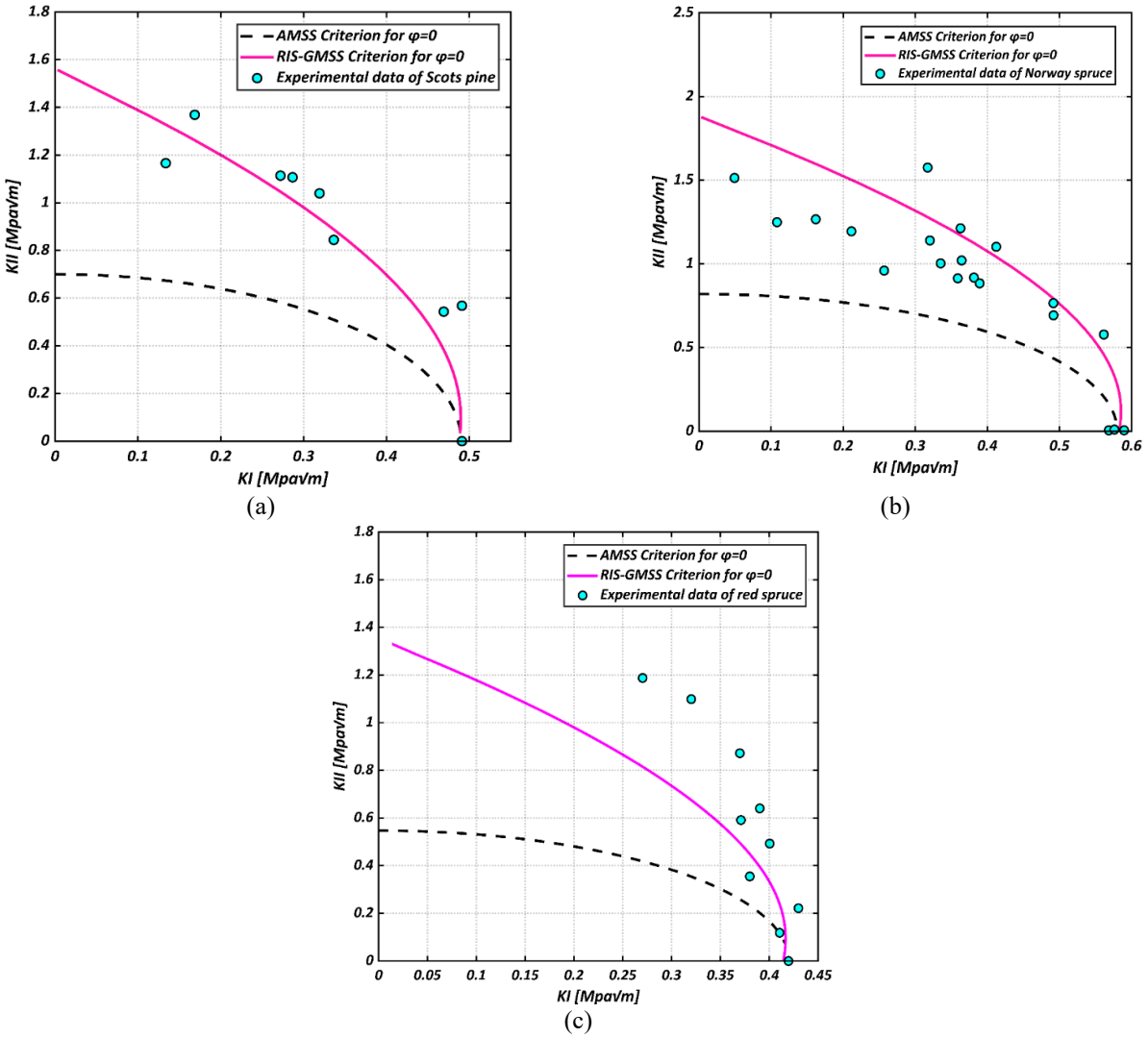

Fig. 10 FLC's of RIS-GMSS and AMSS criteria in comparison with: (a) Scots pine experimental data (Hunt and Croager 1982), (b) Norway spruce experimental data (Jernkvist 2001) and (c) Eastern red spruce experimental data (Mall *et al.* 1983)

Berto, F. (2014), "A brief review of some local approaches for the failure assessment of brittle and quasi-brittle materials", *Adv. Mater. Sci. Eng.*, (2014). https://doi.org/10.1155/2014/930679.

Chen, S., Shi, X. and Qiu, Z. (2011), "Shear bond failure in composite slabs—a detailed experimental study", *Steel Compos. Struct.*, **11**(3), 233-250. http://dx.doi.org/10.12989/scs.2011.11.3.233.

D'Angela, D., Ercolino, M., Bellini, C., Di Cocco, V. and Iacoviello, F. (2020), "Characterisation of the damaging micromechanisms in a pearlitic ductile cast iron and damage assessment by acoustic emission testing", *Fatigue Fract. Eng. M.*, **43**(5), 1038-1050. https://doi.org/10.1111/ffe.13214.

Dall'Asta, A., Dezi, L. and Leoni, G. (2002), "Failure mechanisms of externally prestressed composite beams with partial shear connection", *Steel Compos. Struct.*, **2**(5), 315-330. https://doi.org/10.12989/scs.2002.2.5.315.

Daneshjoo, Z., Shokrieh, M.M. and Fakoor, M. (2018), "A micromechanical model for prediction of mixed mode I/II delamination of laminated composites considering fiber bridging effects", *Theor. Appl. Fract. Mech.*, **94**, 46-56. https://doi.org/10.1016/j.tafmec.2017.12.002.

Di Cocco, V., Iacoviello, F. and Cavallini, M. (2010), "Damaging micromechanisms characterization of a ferritic ductile cast iron", *Eng. Fract. Mech.*, **77**(11), 2016-2023. https://doi.org/10.1016/j.engfracmech.2010.03.037.

Di Cocco, V., Iacoviello, F., Rossi, A. and Iacoviello, D. (2014), "Macro and microscopical approach to the damaging micromechanisms analysis in a ferritic ductile cast iron", *Theor. Appl. Fract. Mech.*, **69**, 26-33. https://doi.org/10.1016/j.tafmec.2013.11.003.

Edlund, J., Lindström, H., Nilsson, F. and Reale, M. (2006), "Modulus of elasticity of Norway spruce saw logs vs. structural lumber grade", *Holz als Roh-und Werkstoff*, **64**(4), 273-279. https://doi.org/10.1007/s00107-005-0091-7.

Fakoor, M. (2017), "Augmented Strain Energy Release Rate (ASER): a novel approach for investigation of mixed-mode I/II fracture of composite materials", *Eng. Fract. Mech.*, **179**, 177-189. https://doi.org/10.1016/j.engfracmech.2017.04.049.

Fakoor, M. and Farid, H.M. (2019), "Mixed-mode I/II fracture criterion for crack initiation assessment of composite materials", *Acta Mechanica*, **230**(1), 281-301. https://doi.org/10.1007/s00707-018-2308-y.

Fakoor, M. and Ghoreishi, S.M.N. (2018), "Experimental and

numerical investigation of progressive damage in composite laminates based on continuum damage mechanics", *Polymer Testing,* **70**, 533-543. https://doi.org/10.1016/j.polymertesting.2018.08.013.

Fakoor, M. and Khansari, N.M. (2016), "Mixed mode I/II fracture criterion for orthotropic materials based on damage zone properties", *Eng. Fract. Mech*., **153**, 407-420. https://doi.org/10.1016/j.engfracmech.2015.11.018.

Fakoor, M. and Khansari, N.M. (2018), "General mixed mode I/II failure criterion for composite materials based on matrix fracture properties", *Theor. Appl. Fract. Mech*., **96**, 428-442. https://doi.org/10.1016/j.tafmec.2018.06.004.

Fakoor, M. and Khezri, M.S. (2020), "A micromechanical approach for mixed mode I/II failure assessment of cracked highly orthotropic materials such as wood", *Theor. Appl. Fract. Mech*., **109**, 102740. https://doi.org/10.1016/j.tafmec.2020.102740.

Fakoor, M. and Rafiee, R. (2013), "Fracture investigation of wood under mixed mode I/II loading based on the maximum shear stress criterion", *Strength Mater*., **45**(3), 378-385. https://doi.org/10.1007/s11223-013-9468-8.

Fakoor, M., Rafiee, R. and Zare, S. (2019), "Equivalent reinforcement isotropic model for fracture investigation of orthotropic materials", *Steel Compos. Struct*., **30**(1), 1-12. https://doi.org/10.12989/scs.2019.30.1.001.

Fakoor, M. and Shahsavar, S. (2020), "Fracture assessment of cracked composite materials: Progress in models and criteria", *Theoretical and Applied Fracture Mech*., **105**, 102430. https://doi.org/10.1016/j.tafmec.2019.102430.

Farid, H.M. and Fakoor, M. (2019), "Mixed mode I/II fracture criterion for arbitrary cracks in orthotropic materials considering T-stress effects", *Theor. Appl. Fract. Mech*., **99**, 147-160. https://doi.org/10.1016/j.tafmec.2018.11.015.

Farid, H.M. and Fakoor, M. (2020), "Mixed mode I/II fracture criterion to anticipate behavior of the orthotropic materials", *Steel Compos. Struct*., **34**(5), 671-679. https://doi.org/10.12989/scs.2020.34.5.671.

Fernandino, D.O., Boeri, R.E., Di Cocco, V., Bellini, C. and Iacoviello, F. (2020a), "Damage evolution during tensile test of austempered ductile iron partially austenized", *Mater. Design Process. Commun*., **2**(4), e157. https://doi.org/10.1002/mdp2.157.

Fernandino, D.O., Di Cocco, V., Boeri, R.E. and Iacoviello, F. (2020b), "Microstrain measurements and damage analysis during tensile loading of intercritical austempered ductile iron", *Fatigue Fract. Eng. M*., **43**(11), 2744-2755. https://doi.org/10.1111/ffe.13346.

Fernandino, D.O., Tenaglia, N., Di Cocco, V., Boeri, R.E. and Iacoviello, F. (2020c), "Relation between microstructural heterogeneities and damage mechanisms of a ferritic spheroidal graphite cast iron during tensile loading", *Fatigue Fract. Eng. M*., **43**(6), 1262-1273. https://doi.org/10.1111/ffe.13221.

Golewski, G.L. (2017a), "Effect of fly ash addition on the fracture toughness of plain concrete at third model of fracture", *J. Civil Eng. Management*, **23**(5), 613-620. https://doi.org/10.3846/13923730.2016.1217923.

Golewski, G.L. (2017b), "Determination of fracture toughness in concretes containing siliceous fly ash during mode III loading", *Struct. Eng. Mech*., **62**(1), 1-9. https://doi.org/10.12989/sem.2017.62.1.001.

Golewski, G.L. (2017c), "Improvement of fracture toughness of green concrete as a result of addition of coal fly ash. Characterization of fly ash microstructure", *Mater. Characterization*, **134**, 335-346. https://doi.org/10.1016/j.matchar.2017.11.008.

Golewski, G.L. (2018), "An assessment of microcracks in the Interfacial Transition Zone of durable concrete composites with fly ash additives", *Compos. Struct*., **200**, 515-520. https://doi.org/10.1016/j.compstruct.2018.05.144.

Golewski, G.L. (2019a), "The influence of microcrack width on the mechanical parameters in concrete with the addition of fly ash: Consideration of technological and ecological benefits", *Constr. Build. Mater*., **197**, 849-861. https://doi.org/10.1016/j.conbuildmat.2018.08.157.

Golewski, G.L. (2019b), "Physical characteristics of concrete, essential in design of fracture-resistant, dynamically loaded reinforced concrete structures", *Mater. Design Process. Commun*., **1**(5), e82. https://doi.org/10.1002/mdp2.82

Golewski, G.L. (2020), "Changes in the fracture toughness under mode II loading of low calcium fly ash (LCFA) concrete depending on ages", *Materials*, **13**(22), 5241. https://doi.org/10.3390/ma13225241.

Golewski, G.L. (2021), "The Beneficial Effect of the Addition of Fly Ash on Reduction of the Size of Microcracks in the ITZ of Concrete Composites under Dynamic Loading", *Energies*, **14**(3), 668. https://doi.org/10.3390/en14030668.

Golewski, G.L. and Gil, D.M. (2021), "Studies of Fracture Toughness in Concretes Containing Fly Ash and Silica Fume in the First 28 Days of Curing", *Materials*, **14**(2), 319. https://doi.org/10.3390/ma14020319.

Hunt, D.G. and Croager, W.P. (1982), "Mode II fracture toughness of wood measured by a mixed-mode test method", *J. Mater. Sci. Lett*., **1**(2), 77-79. https://doi.org/10.1007/BF00731031.

Jernkvist, L.O. (2001a), "Fracture of wood under mixed mode loading: I. Derivation of fracture criteria", *Eng. Fracture Mech*., **68**(5), 549-563. https://doi.org/10.1016/S0013-7944(00)00127-2.

Jernkvist, L.O. (2001b), "Fracture of wood under mixed mode loading: II. Experimental investigation of Picea abies", *Eng. Fracture Mech*., **68**(5), 565-576. https://doi.org/10.1016/S0013-7944(00)00128-4.

Kaman, M.O. and Cetisli, F. (2012), "Numerical analysis of center cracked orthotropic fgm plate: Crack and material axes differ by θ", *Steel Compos. Struct*., **13**(2), 187-206. https://doi.org/10.12989/scs.2012.13.2.187.

Khansari, N.M., Fakoor, M. and Berto, F. (2019), "Probabilistic micromechanical damage model for mixed mode I/II fracture investigation of composite materials", *Theor. Appl. Fract. Mech*., **99**, 177-193. https://doi.org/10.1016/j.tafmec.2018.12.003.

Kollmann, F.F., Kuenzi, E.W. and Stamm, A.J. (2012), Principles of Wood Science and Technology: II Wood Based Materials. Springer Science & Business Media.

Leicester, R.H. (2006), "Application of linear fracture mechanics to notched timber elements", *Progress Struct. Eng. Mater*., **8**(1), 29-37. https://doi.org/10.1002/pse.210.

Mall, S., Murphy, J.F. and Shottafer, J.E. (1983), "Criterion for mixed mode fracture in wood", *J. Eng. Mech*., **109**(3), 680-690. https://doi.org/10.1061/(ASCE)0733-9399(1983)109:3(680).

Marsavina, L., Pop, I.O. and Linul, E. (2019), "Mechanical and fracture properties of particleboard", *Frattura Ed., Integrità Strutturale*, **13**(47), 266-276. https://doi.org/10.3221/IGF-ESIS.47.20.

McKinney, J.M. (1972), "Mixed-mode fracture of unidirectional graphite/epoxy composites", *J. Compos. Mater*., **6**(1), 164-166. https://doi.org/10.1177%2F002199837200600115.

Mirsayar, M.M., Razmi, A. and Berto, F. (2018), "Tangential strain-based criteria for mixed-mode I/II fracture toughness of cement concrete", *Fatigue Fract. Eng. M.*, **41**(1), 129-137. https://doi.org/10.1111/ffe.12665.

Nobile, L., Piva, A. and Viola, E. (2004), "On the inclined crack problem in an orthotropic medium under biaxial loading", *Eng.*

Fract. Mech., **71**(4-6), 529-546. https://doi.org/10.1016/S0013-7944(03)00051-1.

Razavi, S.M.J. and Berto, F. (2019), "A new fixture for fracture tests under mixed mode I/II/III loading", *Fatigue Fract. Eng. M*., **42**(9), 1874-1888. https://doi.org/10.1111/ffe.13033,

Reynolds, T.P., Sharma, B., Serrano, E., Gustafsson, P.J. and Ramage, M.H. (2019), "Fracture of laminated bamboo and the influence of preservative treatments", *Compos. Part B: Eng*., **174**, 107017. https://doi.org/10.1016/j.compositesb.2019.107017.

Rizov, V.I. (2017), "Non-linear study of mode II delamination fracture in functionally graded beams", *Steel Compos. Struct*., **23**(3), 263-271. https://doi.org/10.12989/scs.2017.23.3.263.

Romanowicz, M. (2019), "A non-local stress fracture criterion accounting for the anisotropy of the fracture toughness", *Eng. Fract. Mech*., **214**, 544-557. https://doi.org/10.1016/j.engfracmech.2019.04.033.

Romanowicz, M. and Seweryn, A. (2008), "Verification of a non-local stress criterion for mixed mode fracture in wood", *Eng. Fract. Mech*., **75**(10), 3141-3160. https://doi.org/10.1016/j.engfracmech.2007.12.006.

Ross, R.J. (2010), Wood handbook: wood as an engineering material. USDA Forest Service, Forest Products Laboratory. General Technical Report FPL-GTR-190, 509(5).

Scorza, D., *et al*. (2019), "Size-effect independence of particleboard fracture toughness", *Compos. Struct*., **229**, 111374. https://doi.org/10.1016/j.compstruct.2019.111374.

Saouma, V.E., Ayari, M.L. and Leavell, D.A. (1987), "Mixed mode crack propagation in homogeneous anisotropic solids", *Eng. Fract. Mech*., **27**(2), 171-184. https://doi.org/10.1016/0013-7944(87)90166-4.

Shahsavar, S., Fakoor, M. and Berto, F. (2020), "Verification of reinforcement isotropic solid model in conjunction with maximum shear stress criterion to anticipate mixed mode I/II fracture of composite materials", *Acta Mechanica*, 1-20. https://doi.org/10.1007/s00707-020-02810-8.

Sih, G.C., Paris, P.C. and Irwin, G.R. (1965), "On cracks in rectilinearly anisotropic bodies", *Int. J. Fract. Mech*., **1**(3), 189-203. https://doi.org/10.1007/BF00186854.

Su, R.K.L. and Sun, H.Y. (2003), "Numerical solutions of two-dimensional anisotropic crack problems", *Int. J. Solids Struct*., **40**(18), 4615-4635. https://doi.org/10.1016/S0020-7683(03)00310-X.

Toribio, J. and Ayaso, F.J. (2003), "A fracture criterion for high-strength steel structural members containing notch-shape defects", *Steel Compos. Struct*., **3**(4), 231-242. https://doi.org/10.12989/scs.2003.3.4.231.

Van der Put, T.A.C.M. (2007), "A new fracture mechanics theory for orthotropic materials like wood", *Eng. Fract. Mech*., **74**(5), 771-781. https://doi.org/10.1016/j.engfracmech.2006.06.015.

Wang, D., Lin, L., Fu, F. and Fan, M. (2019), "The softwood fracture mechanisms at the scales of the growth ring and cell wall under bend loading", *Wood Sci. Technol*., **53**(6), 1295-1310. https://doi.org/10.1007/s00226-019-01132-w.

Williams, M.L. (1961), The bending stress distribution at the base of a stationary crack. https://doi.org/10.1115/1.3640470

Wu, E.M. (1967), Application of fracture mechanics to anisotropic plates. https://doi.org/10.1115/1.3607864

Appendix A

The plane of maximum shear stress is shown in Fig. A1 and can be obtained as follows

$$\tau = \frac{\left(\sigma_x - \sigma_y\right)}{2}\sin 2\theta - \sigma_{xy}\cos 2\theta$$

$$\frac{d\tau}{d\theta} = \left(\sigma_x - \sigma_y\right)\cos 2\theta + 2\sigma_{xy}\sin 2\theta = 0 \qquad \text{(A1)}$$

$$\tan 2\theta = -\left(\sigma_x - \sigma_y\right)/2\sigma_{xy}$$

Considering RIS concept, we have

$$\tan 2\theta = \left(\frac{-\left(\frac{K_I}{\gamma_1\sqrt{2\pi r}}p_{11}(\theta) + \frac{K_{II}}{\gamma_1\sqrt{2\pi r}}q_{11}(\theta)\right)}{2\left(\frac{K_I}{\gamma_3\sqrt{2\pi r}}p_{12}(\theta) + \frac{K_{II}}{\gamma_3\sqrt{2\pi r}}q_{12}(\theta)\right)} - \frac{\left(\frac{K_I}{\gamma_2\sqrt{2\pi r}}p_{22}(\theta) + \frac{K_{II}}{\gamma_2\sqrt{2\pi r}}q_{22}(\theta)\right)}{2\left(\frac{K_I}{\gamma_3\sqrt{2\pi r}}p_{12}(\theta) + \frac{K_{II}}{\gamma_3\sqrt{2\pi r}}q_{12}(\theta)\right)} \right) \qquad \text{(A2)}$$

Now, for pure mode I loading condition we have

$$\tan 2\theta_c = \frac{\gamma_1\gamma_3 p_{22}(\theta) - \gamma_2\gamma_3 p_{11}(\theta)}{2\gamma_1\gamma_2 p_{12}(\theta)} \quad \Rightarrow$$

$$\tan 2\theta_c = \left(\frac{\gamma_1\gamma_3(\cos\frac{\theta}{2})(1+\sin\frac{3\theta}{2}\sin\frac{\theta}{2})}{2\gamma_1\gamma_2(\sin\frac{\theta}{2}\cos\frac{\theta}{2}\cos\frac{3\theta}{2})} - \frac{\gamma_2\gamma_3(\cos\frac{\theta}{2})(1-\sin\frac{3\theta}{2}\sin\frac{\theta}{2})}{2\gamma_1\gamma_2(\sin\frac{\theta}{2}\cos\frac{\theta}{2}\cos\frac{3\theta}{2})} \right) \qquad \text{(A3)}$$

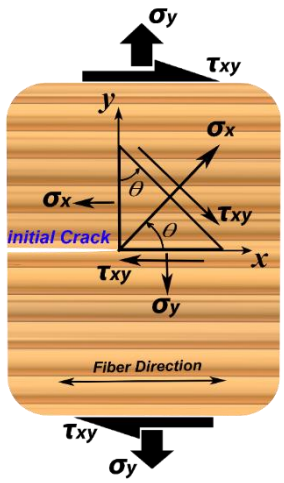

Fig. A1 Plane of maximum shear stress at the crack tip of an orthotropic material

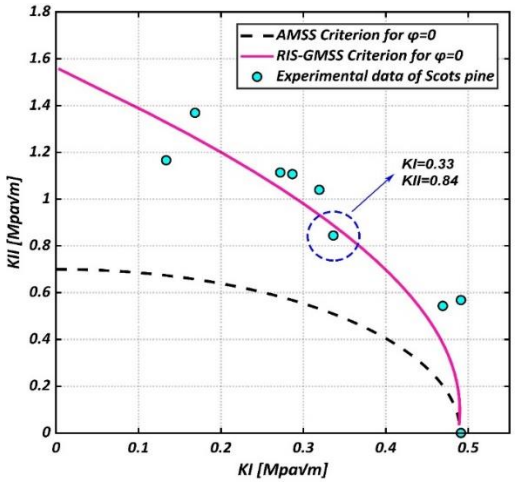

Fig. A2 Critical stress intensity factors for mixed mode case

$$\tan 2\theta_c = \frac{\gamma_1\gamma_3 p_{22}(\theta) - \gamma_2\gamma_3 p_{11}(\theta)}{2\gamma_1\gamma_2 p_{12}(\theta)} \quad \Rightarrow$$

$$\tan 2\theta_c = \left(\frac{\gamma_1\gamma_3(\cos\frac{\theta}{2})(1+\sin\frac{3\theta}{2}\sin\frac{\theta}{2})}{2\gamma_1\gamma_2(\sin\frac{\theta}{2}\cos\frac{\theta}{2}\cos\frac{3\theta}{2})} - \frac{\gamma_2\gamma_3(\cos\frac{\theta}{2})(1-\sin\frac{3\theta}{2}\sin\frac{\theta}{2})}{2\gamma_1\gamma_2(\sin\frac{\theta}{2}\cos\frac{\theta}{2}\cos\frac{3\theta}{2})} \right) \qquad \text{(A3)}$$

For stress state along the fibers ($\theta = 0$), we have

$$\tan 2\theta_c = \infty \quad \Rightarrow \quad \theta_c = \frac{\pi}{4}, -\frac{\pi}{4}, \frac{3\pi}{4}, -\frac{3\pi}{4} \qquad \text{(A4)}$$

And for pure mode II loading condition, we have

$$\tan 2\theta_c = \left(\frac{\gamma_1\gamma_3(\sin\frac{\theta}{2}\cos\frac{\theta}{2}\cos\frac{3\theta}{2})}{2\gamma_1\gamma_2(\cos\frac{\theta}{2})(1-\sin\frac{3\theta}{2}\sin\frac{\theta}{2})} - \frac{\gamma_2\gamma_3(\sin\frac{\theta}{2})(2+\cos\frac{3\theta}{2}\cos\frac{\theta}{2})}{2\gamma_1\gamma_2(\cos\frac{\theta}{2})(1-\sin\frac{3\theta}{2}\sin\frac{\theta}{2})} \right) \qquad \text{(A5)}$$

For stress state along the fibers ($\theta = 0$), we have

$$\tan 2\theta_c = 0 \quad \Rightarrow \quad \theta_c = 0, \pi \qquad \text{(A6)}$$

For a mixed mode case, using Scots pine experimental data (Fig. A2), θ_c can be found as follows

$$\tan 2\theta_c = \frac{-\left[\left(\frac{K_{Ic}}{\gamma_1}\right)-\left(\frac{K_{Ic}}{\gamma_2}\right)\right]}{2\left(\frac{K_{IIc}}{\gamma_3}\right)} = \frac{-\left[\left(\frac{0.33}{14.8}\right)-\left(\frac{0.33}{1}\right)\right]}{2\left(\frac{0.84}{6.8}\right)} = 1.24 \qquad \text{(A7)}$$

$$\Rightarrow \ \theta_c = 25.55$$

Where, $K_{Ic} = 0.33$ & $K_{IIc} = 0.84$.